



A negative feedback loop underlies the Warburg effect



Alok Jaiswal & Raghendra Singh

Aerobic glycolysis, or the Warburg effect, is used by cancer cells for proliferation while producing lactate. Although lactate production has wide implications for cancer progression, it is not known how this effect increases cell proliferation and relates to oxidative phosphorylation. Here, we elucidate that a negative feedback loop (NFL) is responsible for the Warburg effect. Further, we show that aerobic glycolysis works as an amplifier of oxidative phosphorylation. On the other hand, quiescence is an important property of cancer stem cells. Based on the NFL, we show that both aerobic glycolysis and oxidative phosphorylation, playing a synergistic role, are required to achieve cell quiescence. Further, our results suggest that the cells in their hypoxic niche are highly proliferative yet close to attaining quiescence by increasing their NADH/NAD⁺ ratio through the severity of hypoxia. The findings of this study can help in a better understanding of the link among metabolism, cell cycle, carcinogenesis, and stemness.

Otto Heinrich Warburg found that, unlike normal cells, cancer cells use incomplete glycolysis and ferment glucose into lactate¹, even in the presence of oxygen, to proliferate in place of the complete oxidation of glucose using the TCA cycle and oxidative phosphorylation. A definite understanding of the Warburg effect² was not known because complete oxidation appeared to be more efficient than incomplete glycolysis¹ since the latter involves the wastage of glucose carbon excreted as lactate³. Nonetheless, aerobic glycolysis is a general feature of the regulation of cell proliferation both in cancer and normal cells³.

In glycolysis, glucose is oxidized to glyceraldehyde 3-phosphate, which is oxidized to 1,3-bisphosphoglycerate by the enzyme glyceraldehyde 3-phosphate dehydrogenase (GAPDH)³. Further, in this process, NADH is produced, although NAD⁺ is required for the GAPDH activity³ to carry on the glycolysis. Thus, in the cytoplasm, NAD⁺ needs to be regenerated from NADH. There are three ways NAD⁺ can be regenerated from NADH in the cytosol: 1. The malate-aspartate shuttle (MAS) 2. The glycerol 3-phosphate shuttle (G3PS) 3. The reduction of pyruvate to lactate by lactate dehydrogenase (LDH)³. MAS and G3PS help translocate the reducing power of glucose to oxidative phosphorylation in the mitochondria³. In contrast, the reduction of pyruvate to lactate does not participate in the running of oxidative phosphorylation³. Recently, it has been found that the driving force for aerobic glycolysis is the saturation of the NADH shuttles of MAS and G3PS toward oxidative phosphorylation³. In contrast, our model and analysis suggest a synergistic relation between aerobic glycolysis and oxidative phosphorylation.

Cancer cells have a high glycolysis rate, which occurs when the NADH/NAD⁺ ratio is low because a high NADH/NAD⁺ ratio inhibits GAPDH⁴. Further, NAD⁺ is produced from NADH by the cytosolic malate dehydrogenase 1 (MDH1)⁵, decreasing NADH/NAD⁺ ratio in the cytoplasm. Furthermore, human tumors overexpress MDH1, and the MDH1 expression correlates with poor prognosis⁵, suggesting a role of the decreased NADH/NAD⁺ ratio in tumor progression.

BRCA1 transactivates the cyclin-dependent kinase inhibitor CDKN1A⁶. On the other hand, CtBP, through the CtIP-CtBP-BRCA1 repressor complex causes CDKN1A promoter deacetylation, repressing CDKN1A transcription and promoting the G1-S transition of cells⁷. Further, NADH is required for the CtBP dimerization and the formation of the repression complex involving the dimeric CtBP⁸. Thus, NADH promotes the cell cycle progression through the dimeric CtBP by repressing CDKN1A. Besides the cell cycle, a link between aerobic glycolysis, NADH-CtBP, and TP53 has been established⁴. NADH, through the dimeric CtBP, causes TP53 accumulation⁴. Thus, an increase in NADH concentration may cause apoptosis through TP53 accumulation. Similarly, a decrease in CDKN1A, which can be caused by the repression of CDKN1A by NADH-CtBP, may induce apoptosis⁹. Thus, NADH causes both cell cycle progression and apoptosis (Fig. 1a). Further, one of the reasons why cancer cells supplement oxidative phosphorylation with aerobic glycolysis is that the cytoplasmic NADH directly controls the cell cycle and apoptosis, the processes that control cell proliferation directly through the repression of CDKN1A and accumulation of TP53 by NADH-CtBP.

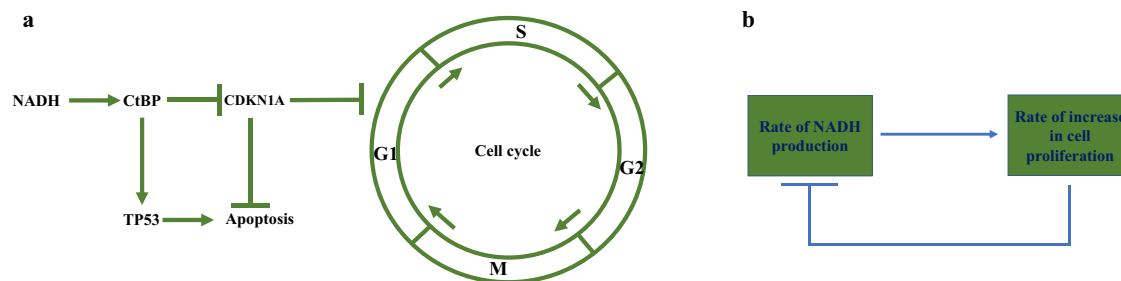


Fig. 1 | NADH controls cell cycle and cell proliferation. **a** The regulation of cell cycle and apoptosis by NADH through CtBP. **b** The negative feedback loop between the rate of NADH production and the rate of increase in cell proliferation.

However, how glycolysis causes cell proliferation while producing lactate lacked clarity. Our results show that a reduction in NADH/NAD⁺ ratio, while NADH-CtBP causes the cell cycle progression, increases cell proliferation. This is due to a negative feedback loop (NFL) between the rate of increase in cell proliferation and the rate of increase in cytoplasmic NADH concentration (Fig. 1b), generating an inverse relationship between NADH and cell proliferation (Eq. 17, Methods section). Further, the results show that cell proliferation is higher if either the effectiveness of NADH increase in the cytoplasm through glycolysis is lower and/or pyruvate-to-lactate conversion is higher and/or flux of NADH and NADH-equivalent to mitochondria is higher. Thus, retention of the reducing power of NADH in the cytoplasm is detrimental to cell proliferation, even though NADH is involved in cell cycle progression. Further, we show that oxidative phosphorylation and aerobic glycolysis have a synergistic relation. Furthermore, aerobic glycolysis serves as an amplifier of oxidative phosphorylation in increasing cell proliferation when NADH/NAD⁺ ratio decreases and in keeping a high concentration of NAD⁺ in cells. The paper is organized as follows:

First, the result section is presented. Then, the discussion section is presented. In the result section, first, we derive the condition for cell quiescence. This condition brings up a non-dimensional number that we define as the inverse of potential-to-proliferation-increase (IPPI). When IPPI=1, cells are not quiescent. Next, we present the effect of decreasing NADH/NAD⁺ ratio on cell proliferation when IPPI>1. Here, we also present evidence from other studies to show that the reduction of NADH/NAD⁺ ratio is a general mechanism found in both cancer and normal cells, through which cells increase their proliferation. In IPPI, glycolysis, oxidative phosphorylation, and pyruvate-to-lactate conversion reactions (i.e., aerobic glycolysis) are involved. We present evidence that oxidative phosphorylation and pyruvate-to-lactate conversion reaction play a synergistic role in increasing cell proliferation when NADH/NAD⁺ ratio decreases. Then, we return to cell quiescence and show that both oxidative phosphorylation and pyruvate-to-lactate conversion reaction are essential for attaining cell quiescence, and aerobic glycolysis works as an amplifier of oxidative phosphorylation. In the discussion section, we discuss how metabolism, cell cycle, and apoptosis are linked. Further, we discuss the implication of our study for solid tumors in hypoxic conditions and cancer cell stemness and how lactate production profoundly affects different aspects of solid tumors, causing cancer progression. Finally, the method section is presented.

Results

The condition of cell quiescence

Cancer cells have poor DNA damage response and are sensitive to drugs that cause DNA damage in these cells during cell cycle progression¹⁰. On the other hand, cancer stem cells exit the cell cycle and are quiescent, causing drug resistance¹¹⁻¹³. Further, normal cells, during differentiation, exit the cell cycle and become quiescent¹⁴. Furthermore, quiescence is a property of stem cells, preventing their functional exhaustion¹⁵. Below, we derive the condition for cell quiescence:

From Eq. 15 (Methods section), at the baseline and steady state,

$$\frac{k_3}{k_4 + C_{p0}} - k_{d2}N_0 = 0 \tag{1}$$

where, k_3 is NADH flux from glycolysis and k_4 is the fold decrease in this flux due to the pyruvate-to-lactate conversion reaction. N_0 is the baseline NADH concentration in the cytoplasm and C_{p0} is cell proliferation, which is defined as the fold increase in the number of cells from a single cell, at the baseline.

Thus, from Eq. 1,

$$\frac{k_3}{k_4 k_{d2} N_0} = \frac{k_4 + C_{p0}}{k_4} \geq 1 \tag{2}$$

The equality in $\frac{k_4 + C_{p0}}{k_4} \geq 1$ in Eq. 2 is when $C_{p0} = 0$, and cells are quiescent at the baseline. Thus, for the quiescent cells at the baseline, the ratio IPPI = $\frac{k_3}{k_4 k_{d2} N_0} = 1$.

A decrease in NADH/NAD⁺ ratio increases the cell proliferation

Our model shows that a decrease in NADH/NAD⁺ ratio, which may happen due to changes in the kinetic parameters of the cell cycle and apoptosis according to Eq. 16 (Methods section), increases cell proliferation (Fig. 2a) according to Eq. 18 (Methods section). Thus, the cancer cells may reset their NADH/NAD⁺ ratio to attain a higher proliferation rate.

The above conclusion is in agreement with experimental findings in both cancer and normal cells. For example, in cancer cells, which are usually in a high glycolytic state, the NADH/NAD⁺ ratio is low⁴. In this context, SRC activity reduces the NADH/NAD⁺ ratio by activating NADH ubiquinone-oxidoreductase¹⁶. Notably, SRC is well known to cause cell proliferation^{17,18}. Further, SRC activity has been implicated in many types of cancers^{19,20}, implicating the reduction of the NADH/NAD⁺ ratio in cancers.

On the other hand, in the normal fetal liver hematopoietic stem cells (FL-HSCs), the MDH1-mediated malate-aspartate NADH shuttle reduces the cytoplasmic NADH/NAD⁺ ratio²¹ and causes rapid proliferation of the cells²¹.

Further, memory characteristics of innate immunity protect against secondary infection after primary exposure to infections or vaccinations²². Monocytes trained with the β -glucan component of *Candida albicans* upregulated glycolysis and lactate production²² and decreased the NADH/NAD⁺ ratio. Interestingly, β -glucan from *Grifola frondosa* caused the proliferation of macrophages²³, and cell cycle activation of β -glucan-trained cells has been observed²⁴. Further, β -glucan induces the proliferation and activation of monocytes²⁵. Thus, in general, a decrease in NADH/NAD⁺ ratio has been implicated in increasing the proliferation rate of cells. Therefore, the reduction in NADH/NAD⁺ ratio is a general mechanism to attain a higher cell proliferation through aerobic glycolysis (Fig. 2a).

In contrast, if the NADH/NAD⁺ ratio increases, cell proliferation decreases (Fig. 2b). In this context, SRC kinase phosphorylates the mitochondrial NADH ubiquinone-oxidoreductase, preserving its activity¹⁶.

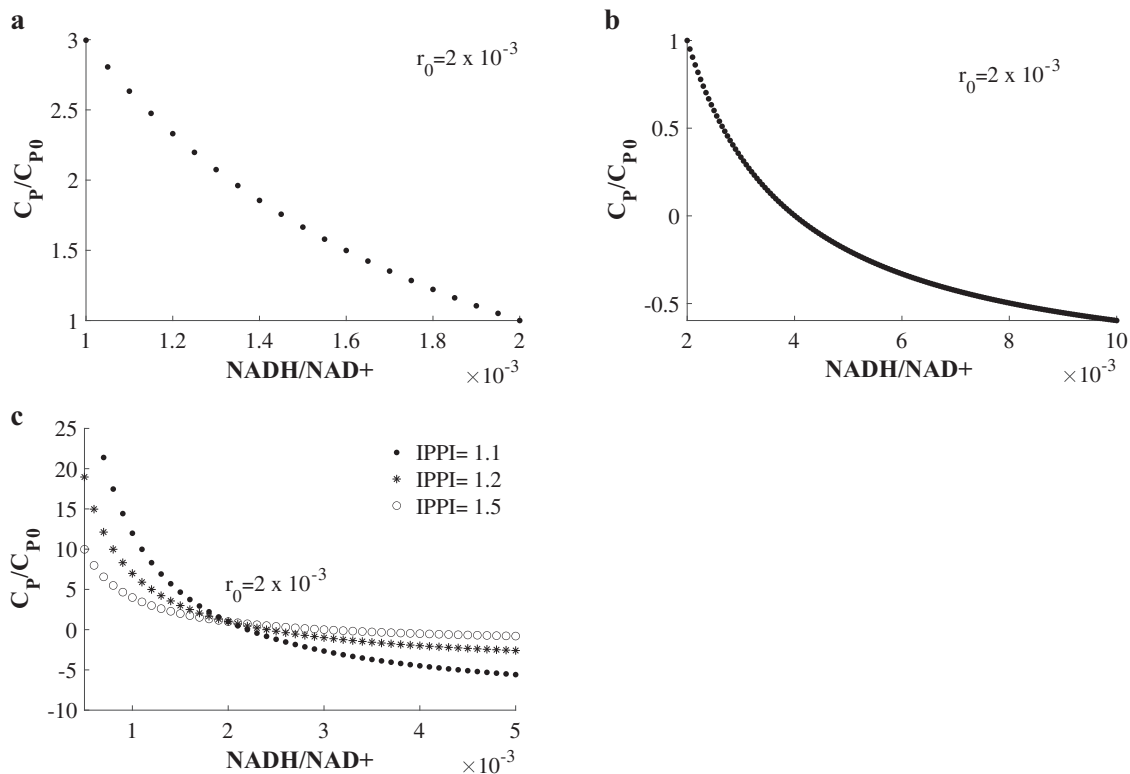


Fig. 2 | Effect of variation in NADH/NAD+ ratio on the relative cell proliferation. **a** The variation in the relative cell proliferation (C_p/C_{p0}) as a function of NADH/NAD+ ratio for IPPI = 2.0, when NADH/NAD+ ratio, r , is less than r_0 , which is the baseline NADH/NAD+ ratio. **b** The variation in the relative cell

proliferation (C_p/C_{p0}) as a function of NADH/NAD+ ratio for IPPI = 2.0, when NADH/NAD+ ratio, r , is more than r_0 , which is the baseline NADH/NAD+ ratio. **c** The variation in the relative cell proliferation (C_p/C_{p0}) when NADH/NAD+ ratio, r , is varied for different values of the ratio $IPPI = \frac{k_3}{k_4 k_{d2} N_0}$.

On the other hand, the inhibition of SRC blocks this activity¹⁶. Further, blocking the activity of NADH ubiquinone-oxidoreductase increases the cytoplasmic NADH/NAD+ ratio by reducing the NADH shuttles, MAS and G3PS, to mitochondria. Thus, the inhibition of SRC reduces the proliferation of cells by increasing the NADH/NAD+ ratio in cells.

Similarly, Optic Atrophy 1 (OPA1), which regulates cristae shape in mitochondria, controls the TCA cycle in T helper 17 (T_H17) cells²⁶. In agreement with the antagonistic effect of the increase in NADH/NAD+ ratio on cell proliferation, OPA1 deletion increased NADH/NAD+ ratio in T_H17 cells, impaired IL-17 production, and decreased their proliferation²⁶.

Moreover, increasing the NADH/NAD+ ratio further can cause cell proliferation to turn negative (Fig. 2b). Therefore, increasing the NADH/NAD+ ratio may be useful in anti-cancer therapy. Interestingly, the growth of the cells, whose proliferation increases more when the NADH/NAD+ ratio is decreased relative to the baseline NADH/NAD+ ratio r_0 , reduces faster and turns more negative when the NADH/NAD+ ratio is increased relative to the baseline NADH/NAD+ ratio r_0 (Fig. 2c). Thus, the cells with a lower value of the ratio $IPPI = \frac{k_3}{k_4 k_{d2} N_0}$, in Eq. 18 (Methods section), are more amenable to anti-cancer therapy that increases their NADH/NAD+ ratio (Fig. 2c).

The effect of $IPPI = \frac{k_3}{k_4 k_{d2} N_0}$ ratio when $IPPI \neq 1$

When the ratio $IPPI = \frac{k_3}{k_4 k_{d2} N_0}$, which is higher than unity according to inequality 2, is comparable to unity, the increase in cell proliferation, $\frac{C_p}{C_{p0}}$, due to a reduction in NADH/NAD+ ratio, depends on the $\frac{k_3}{k_4 k_{d2} N_0}$ (Fig. 3a). In contrast, if $IPPI = \frac{k_3}{k_4 k_{d2} N_0} \gg 1$, the $\frac{C_p}{C_{p0}}$ is independent of the ratio $\frac{k_3}{k_4 k_{d2} N_0}$ (Fig. 3b). In the subsections below, we analyze the effect of different variables in the ratio $\frac{k_3}{k_4 k_{d2} N_0}$ on cell proliferation when the ratio, $\frac{k_3}{k_4 k_{d2} N_0}$ is comparable to unity.

A lower effectiveness in increasing the NADH concentration by glycolysis increases cell proliferation more when the NADH/NAD+ ratio decreases. The variable k_3 , from Eq. 15 (Methods section), is the incoming NADH flux from the upstream steps of glycolysis. From Fig. 3a, the increase in cell proliferation, when NADH/NAD+ ratio decreases, is higher for the lower values of IPPI, $\frac{k_3}{k_4 k_{d2} N_0}$. Thus, a lower value of k_3 increases the proliferation more when the NADH/NAD+ ratio decreases. This is consistent with the increase in the activity of GAPDH by NAD+ when the effectiveness of increasing the cytoplasmic NADH concentration decreases due to a lower value of k_3 .

Pyruvate-to-lactate conversion reaction helps achieve a higher cell proliferation when the NADH/NAD+ ratio decreases. Since a lower magnitude of the non-dimensional number $IPPI = \frac{k_3}{k_4 k_{d2} N_0}$, increases the proliferation more (Fig. 3a), a higher magnitude of k_4 , which is the fold decrease in NADH flux due to pyruvate-to-lactate conversion reaction, increases the proliferation more when NADH/NAD+ decreases (Fig. 3a). Thus, the pyruvate-to-lactate conversion reaction or the Warburg effect helps cells attain a higher cell proliferation by decreasing their NADH/NAD+ ratio.

The flow of the reducing power toward oxidative phosphorylation increases the proliferation more when the NADH/NAD+ ratio decreases. Similarly, in the ratio $\frac{k_3}{k_4 k_{d2} N_0}$, a higher value of the variable k_{d2} , which, according to Eq. 15 (Methods section), is related to the flux of NADH and NADH-equivalent toward oxidative phosphorylation and TCA cycle, also increases cell proliferation more when NADH/NAD+ decreases according to Fig. 3a.

Thus, the upstream steps in glycolysis, which increase NADH, are unhelpful in promoting relative cell proliferation, while the downstream steps of pyruvate-to-lactate conversion and oxidative phosphorylation,

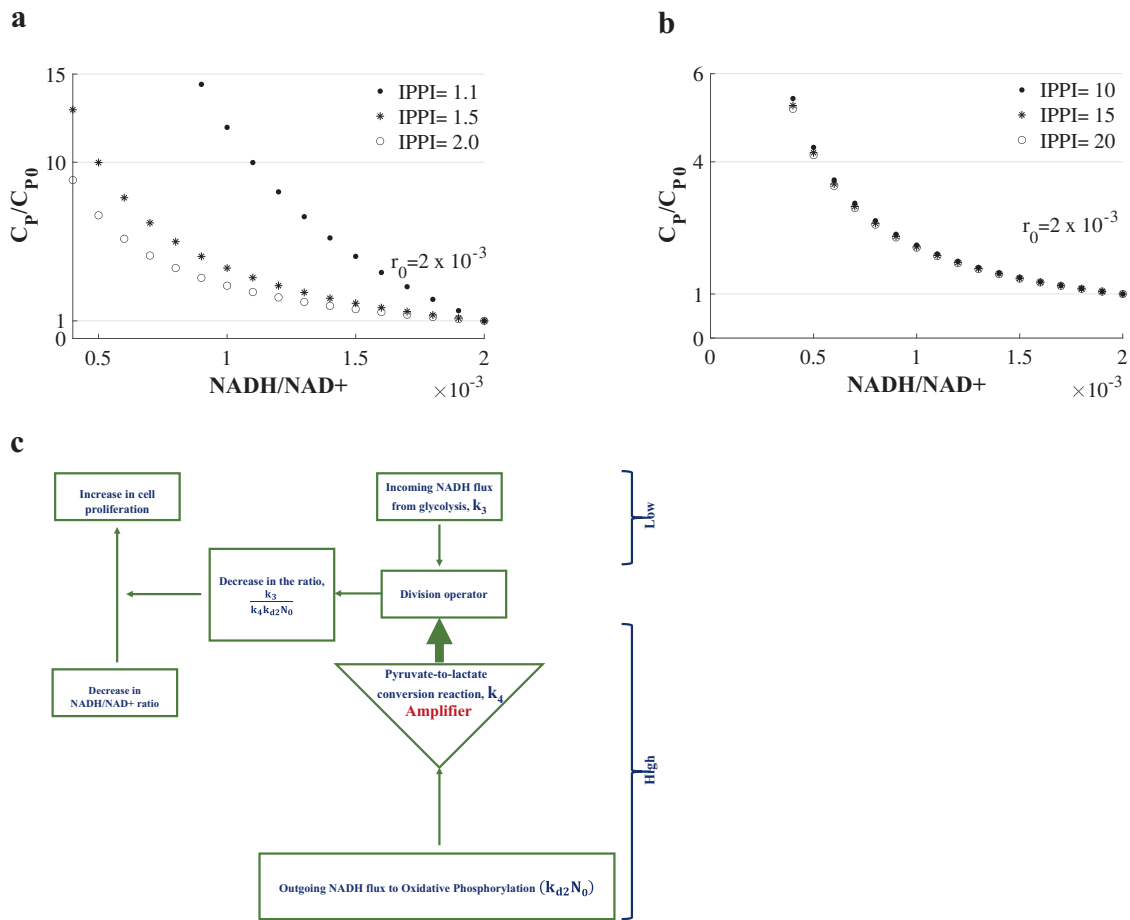


Fig. 3 | A decrease in NADH/NAD+ ratio increases the relative cell proliferation more when the ratio IPPI is lower and comparable to unity, for IPPI > 1. a The variation in the relative cell proliferation (C_p/C_{p0}) when NADH/NAD+ ratio, r , is varied for different values of the ratio $IPPI = \frac{k_3}{k_4 k_{d2} N_0}$ for $r < r_0$ i.e. for a decrease in the NADH/NAD+ ratio. The ratio, IPPI, is comparable to unity. **b** The variation in the

relative cell proliferation (C_p/C_{p0}) when NADH/NAD+ ratio, r , is varied for different values of the ratio $IPPI = \frac{k_3}{k_4 k_{d2} N_0}$ for $r < r_0$ i.e. for a decrease in the NADH/NAD+ ratio. The ratio, IPPI, is much higher than unity. **c** Pyruvate-to-lactate conversion reaction works as an amplifier of oxidative phosphorylation in increasing the relative proliferation rate when the NADH/NAD+ ratio decreases.

which consume NADH, promote the relative increase in cell proliferation. Further, the cytoplasmic NADH is detrimental to cell proliferation even though it causes cell cycle progression through CtBP.

In the ratio $IPPI, \frac{k_3}{k_4 k_{d2} N_0}$, the term $k_{d2} N_0$ is the flux of NADH and NADH-equivalent to mitochondria (Eq. 15, Methods section). This flux is amplified by k_4 , the fold decrease in the incoming NADH flux from glycolysis due to the pyruvate-to-lactate conversion reaction, and the higher value of $k_4 k_{d2} N_0$ increases the proliferation rate more when NADH/NAD+ ratio decreases (Fig. 3a and c). Thus, the pyruvate-to-lactate conversion reaction serves as an amplifier of oxidative phosphorylation in promoting relative cell proliferation (Fig. 3c).

Cell quiescence requires a higher level of oxidative phosphorylation and/or aerobic glycolysis

From Eq. 17 (Methods section), for the cell quiescence at the baseline (i.e. $C_{p0} = 0$), the NADH concentration is:

$$N_0 = \frac{k_3}{k_{d2} k_4} \tag{3}$$

Further, from Eq. 3, for the quiescence at the baseline, either the oxidative phosphorylation (k_{d2}) or the lactate production (k_4) should be high so that quiescence can be attained at a moderate level of NADH and

not at an exorbitant level of NADH, which can cause apoptosis in the cells.

If $k_{d2} = 0$ or $k_4 = 0$, i.e., if the cells hadn't had the oxidative phosphorylation or the lactate production, from Eq. 3, to achieve quiescence, the cell would need an infinite concentration of NADH. Thus, in the absence of oxygen or pyruvate-to-lactate conversion reaction, the cell will never achieve quiescence. In agreement, it has been found that respiration is essential for maintaining the quiescence of adult hematopoietic stem cells²⁷. Further, in agreement with the above analysis, the overexpression of LDH in muscle stem cells causes their quiescence²⁸. In contrast, isocitrate dehydrogenase (IDH) mutation in glioma causes lactate dehydrogenase LDH-A silencing²⁹ and the glioma cells do not attain quiescence³⁰. Interestingly, IDH mutant gliomas have a better prognosis²⁹ since they are not quiescent, and quiescence is related to the stemness of cancer cells. In contrast, gliomas that do not have IDH mutation express higher levels of PROM1 and SOX2, the stem cell markers³¹. PROM1 expression causes quiescence in glioma cells³². Thus, LDH-A activity in IDH-wild-type gliomas is involved in conferring stemness and quiescence by increasing lactate production (k_4). Therefore, aerobic glycolysis is a general mechanism that also incorporates the attainment of quiescence.

The above analysis is for the quiescence of the cells at the baseline when Eq. 18 (Methods section) is not applicable because its denominator becomes zero, and instead, we used Eq. 17 (Methods section). On the other hand, if the baseline cells are proliferating, Eq. 18 is applicable. For the quiescence of

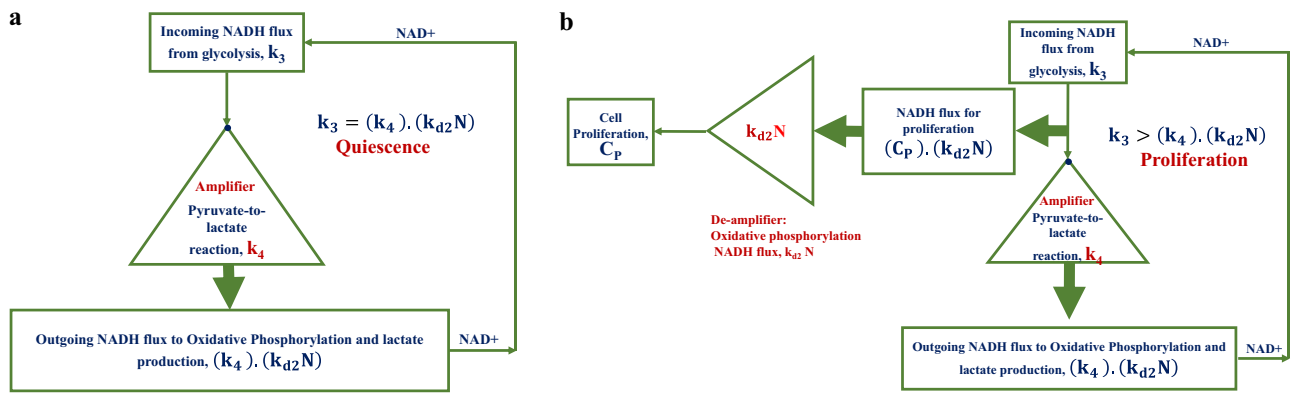


Fig. 4 | The conditions for cell quiescence and cell proliferation. **a** The condition, $k_3 = k_4 k_{d2} N_0$, is satisfied for the cell quiescence. Further, the pyruvate-to-lactate conversion reaction works as an amplifier in maintaining the high concentration of NAD^+ in cells. **b** The condition, $k_3 > k_4 k_{d2} N_0$, is satisfied for cell proliferation. The

difference, $k_3 - k_4 k_{d2} N_0$, is the NADH flux for cell proliferation through CtBP. This flux is de-amplified by the NADH flux for the oxidative phosphorylation to give the cell proliferation C_p .

these cells (i.e. $C_p = 0$) at the NADH/ NAD^+ ratio of r , from Eq. 18 (Methods section),

$$\left(\frac{k_3}{k_4 k_{d2} N_0}\right) \left(\frac{r+1}{r_0+1}\right) \frac{r_0}{r} - 1 = 0 \tag{4}$$

where, r_0 is the baseline NADH/ NAD^+ ratio. Since in eukaryotic cells $r \ll 1$ and $r_0 \ll 1$ ³³,

$$\frac{r+1}{r_0+1} \approx 1$$

Then, from Eq. 4, to attain quiescence at an NADH/ NAD^+ ratio of r

$$\frac{r}{r_0} \approx \frac{k_3}{k_4 k_{d2} N_0} \tag{5}$$

From Eq. 5 and inequality 2, for attaining quiescence at r by the cells whose baseline is proliferating

$$\frac{r}{r_0} = \frac{k_3}{k_4 k_{d2} N_0} > 1 \tag{6}$$

Thus, from inequality 6, for the quiescence of the proliferating cells, since the ratio, $\frac{r}{r_0}$, should be higher than unity, the proliferating cells have to increase their NADH/ NAD^+ ratio to achieve quiescence. In contrast, cancer cells decrease their NADH/ NAD^+ ratio, although the hypoxic environment of solid tumors brings near quiescence in cancer cells by increasing the NADH/ NAD^+ ratio³⁴.

Aerobic glycolysis works as an amplifier of oxidative phosphorylation to maintain a high level of NAD^+ in cells

From Eq. 6, for quiescence (Supplementary Information 1 and Supplementary Movie 1)

$$k_3 = (k_4) \cdot (k_{d2} N) \tag{7}$$

or

$$\text{Incoming NADH flux from glycolysis} = \text{product of the fold reduction in the incoming NADH flux from glycolysis due to the pyruvate-to-lactate conversion reaction } (k_4) \text{ and the outgoing flux of NADH to oxidative phosphorylation } (k_{d2} N) \tag{8}$$

In Eq. 7 or 8, the outgoing NADH flux to oxidative phosphorylation ($k_{d2} N$) is amplified by the lactate production reaction (k_4) (Fig. 4a). Thus, the lactate production reaction works as an amplifier to maintain a high concentration of NAD^+ in cells (Fig. 4a).

On the other hand, for the proliferative cells, from Eq. 18 (Methods section),

$$\left(\frac{k_3}{k_4 k_{d2} N_0}\right) \left(\frac{r+1}{r_0+1}\right) \frac{r_0}{r} - 1 > 0 \tag{9}$$

Since, $\frac{r+1}{r_0+1} \approx 1$

From Eq. 9,

$$\frac{r}{r_0} < \frac{k_3}{k_4 k_{d2} N_0} \tag{10}$$

From Eq. 10 (Supplementary Information 2), for proliferating cells

$$k_3 > (k_4) \cdot (k_{d2} N) \tag{11}$$

or

$$\text{Incoming NADH flux from glycolysis} > \text{Product of the fold reduction in the incoming NADH flux from glycolysis due to the pyruvate-to-lactate conversion reaction } (k_4) \text{ and the outgoing flux of NADH to oxidative phosphorylation } (k_{d2} N) \tag{12}$$

From inequalities 11 or 12, we infer that the extra incoming NADH flux from glycolysis is used for proliferation (Fig. 4b) through CtBP (Supplementary Movie 2).

From Eq. 15 (Methods section), at the steady state,

$$(C_p) \cdot (k_{d2}N) = k_3 - (k_4) \cdot (k_{d2}N) \quad (13)$$

Thus, the outgoing NADH flux for proliferation through CtBP is $C_p \cdot (k_{d2}N)$ (Eq. 13 and Fig. 4b). Further, the cell proliferation C_p is obtained after the conversion of this flux into cell proliferation with the help of a de-amplifier, which is the NADH flux ($k_{d2}N$) to oxidative phosphorylation (Left-hand side of Eq. 13 and Fig. 4b).

Furthermore, since the effect of a decrease in NADH concentration is multiplied by k_{d2} and k_4 (the term $(k_4) \cdot (k_{d2}N)$ in the right-hand side of Eq. 13), the effect of the decrease in NADH/NAD+ ratio in increasing the relative cell proliferation is promoted by both the oxidative phosphorylation and the pyruvate-to-lactate conversion reaction (Supplementary Movie 2). Moreover, the pyruvate-to-lactate conversion reaction amplifies the effect of oxidative phosphorylation in increasing the relative cell proliferation (Fig. 4b) when the NADH/NAD+ ratio decreases through the term, $(k_4) \cdot (k_{d2}N)$, in Eq. 13 (Supplementary Movie 2).

Further, although the outgoing NADH flux, $(C_p) \cdot (k_{d2}N)$, for proliferation causes proliferation through CtBP, it is de-amplified by oxidative phosphorylation (Left-hand side of Eq. 13 and Fig. 4b). Thus, oxidative phosphorylation couples with the cell cycle progression caused by NADH-CtBP.

Discussion

We found that higher rates of oxidative phosphorylation and aerobic glycolysis are required for attaining both a higher cell proliferation, when the NADH/NAD+ ratio decreases, and quiescence. Thus, the same cellular processes are required for both the progression of the cell cycle and the exit from it. Further, we found a non-dimensional number, which we define as the inverse of potential-to-proliferation-increase (IPPI), that regulates cell proliferation. If this number is unity, cells exit from the cell cycle and become quiescent. In contrast, if this number is higher than unity, cells proliferate. The lower magnitude of this number implies a higher proliferation rate. Our model and analysis elucidate the link between metabolism and cell cycle and may be important in understanding how cancer cells regulate their proliferation and devising strategies to increase the NADH/NAD+ ratio in these cells to reduce their proliferation and cause apoptosis in these cells.

NADH concentration is not an independent variable but is controlled by cell proliferation through the cell cycle and apoptosis (Eq. 16, Methods section) involving NADH-CtBP. Indeed, a decrease in the cytosolic NADH/NAD+ ratio decreases the activation of MAPK8 and BAX, inhibiting the apoptotic pathways³⁵. In contrast, an increase in the NADH/NAD+ ratio has been shown to cause TP53 accumulation⁴ and a decrease in CDKN1A level⁷, causing apoptosis^{9,36}. Thus, varying the NADH/NAD+ ratio in the cell affects the cell cycle and apoptosis and vice versa.

The environment within a solid tumor is hypoxic, which reduces oxidative phosphorylation or, in our analysis, reduces k_{d2} in Eq. 15 (Methods section), raising the term $\frac{k_3}{k_4 k_{d2} N_0}$ or the right-hand side of Eq. 6, $\frac{r}{r_0} = \frac{k_3}{k_4 k_{d2} N_0}$, required to be satisfied by the cells to attain quiescence, thus, attaining some degree of proliferation. Further, hypoxia has been shown to increase NADH/NAD+ ratio³⁴, satisfying the condition $\frac{r}{r_0} > 1$ in inequality 6, thus, attaining a relative quiescence. Therefore, hypoxia creates a competition between proliferation and quiescence by increasing both sides of Eq. 6, $\frac{r}{r_0} = \frac{k_3}{k_4 k_{d2} N_0}$. Consequently, in the hypoxic zone, cells are proliferative but close to attaining quiescence. Further, the more severe the hypoxia, i.e., the less the oxidative phosphorylation (i.e., the lower the value of k_{d2}), the more the value of k_4 in Eq. 6, i.e., the higher may be the lactate production, to keep Eq. 6, $\frac{r}{r_0} = \frac{k_3}{k_4 k_{d2} N_0}$, nearly satisfied, and thus, the competition between proliferation and quiescence continues through an increase in both hypoxia and lactate production controlling the ratio $\frac{k_3}{k_4 k_{d2} N_0}$ and satisfying the condition $\frac{r}{r_0} = \frac{k_3}{k_4 k_{d2} N_0}$. Therefore, at the center, assumed at a point of highest

hypoxia in the solid tumor, the lactate production may be the highest, and there may be a gradient of lactate from the presumed center to the surface.

Interestingly, since from Eq. 6 for the quiescence of proliferating cells the condition $\frac{r}{r_0} = \text{IPPI} > 1$ needs to be satisfied and since cells have a higher proliferation rate when IPPI is lower and close to unity, when IPPI is near 1, the cells under hypoxia are both highly proliferative (Fig. 3a) and closer to attaining quiescence because they have to minimally increase their NADH/NAD+ ratio to meet the condition $\frac{r}{r_0} > 1$ and satisfy the condition $\frac{r}{r_0} = \text{IPPI} > 1$ for attaining quiescence. Further, since hypoxia increases the NADH/NAD+ ratio³⁴, the proliferative cells need to increase the level of hypoxia to attain quiescence. Thus, the cells at the presumed center of solid tumors, where hypoxia is the maximum, may be quiescent.

Further, the quiescence caused by hypoxic conditions may increase the stability of both cancer cells and hematopoietic stem cells residing in their respective hypoxic niche. Interestingly, the quiescence in hematopoietic stem cells is caused by TP53³⁷, which accumulates due to increased NADH-CtBP⁴ under hypoxia as hypoxia increases the NADH/NAD+ ratio in cells³⁴. Similarly, the quiescence in cancer cells is caused by TP53-responsive miRNAs, miRNA-27b-3p and miRNA-455-3p, which increase Cdk inhibitor CDKN1B levels³⁸. On the other hand, CDKN1A, another Cdk inhibitor downstream of TP53, is redundant in causing cell quiescence³⁹. Notably, we found that IPPI = 1 is a general condition for cell quiescence. Thus, regardless of how it is implemented by the cell cycle, cell quiescence is caused by metabolism, which creates the overriding condition for it.

Further, the lactate at the surface of the solid tumor causes angiogenesis by the lactate-mediated activation of the RAF-ERK pathway through an oxygen-regulated protein NDRG3⁴⁰. Angiogenesis brings glucose and oxygen to the surface and inside of a solid tumor, and these two diffuse from outside to inside of the tumor. Further, the lactate at the surface creates an immunosuppressive environment surrounding the tumor⁴¹. Furthermore, the cells at the presumed center of the solid tumors have autophagy due to severe hypoxia^{42,43}. Since quiescence and autophagy⁴⁴⁻⁴⁶ are properties of stem cells⁴⁷, and hypoxia stimulates stemness and epithelial-to-mesenchymal transition⁴⁸⁻⁵⁰ along with quiescence and autophagy, these cells in a severe hypoxic zone around the presumed center may have a higher degree of stemness. Thus, the location of cells near the presumed center of a solid tumor may be partly responsible for their stemness.

Our study suggests that the pyruvate-to-lactate conversion reaction is an amplifier of oxidative phosphorylation (OXPHOS) and the Warburg effect may not be a specific phenomenon of cancer cells. The cells have two degrees of freedom through tuning between aerobic glycolysis and OXPHOS, lowering the NADH/NAD+ ratio, and achieving a higher proliferation rate. This suggestion is supported by observation in cell lines. For example, some cell lines exhibit both high oxygen-consuming rate (OCR) and extracellular acidification rate (ECAR), and display fast proliferation, such as the MCF7 cell line, while very few cell lines may display a similar fast cell proliferation but with relatively lower OCR and higher ECAR values such as PC3. In fast proliferative cells, the high glycolytic rate is coupled with high OXPHOS activity. In a simple model, the high glycolytic rate feeds abundant substrate to de-novo synthesis of nuclear acids and lipids, essential for producing new cells. The abundant NADH production from the TCA cycle powers the electron transport chain, pentose phosphate pathway, and lipid synthesis. On the other hand, under unfavorable conditions, such as mitochondrial dysfunction, even though some cancer cells can survive with limited mitochondrial functions, their proliferation speed can be significantly impaired.

In summary, the paper showed that a negative feedback loop (Methods section) is at the core of the Warburg effect and provided an in-depth insight into this effect. Further, our results suggest that cells in a hypoxic environment are highly proliferative yet close to attaining quiescence by increasing their NADH/NAD+ ratio through the increase in the intensity of hypoxia. Our model and analysis help us understand the role of aerobic glycolysis in cell proliferation, quiescence, and other important aspects of solid tumors.

Methods

The basis for a negative feedback loop between the rate of NADH production and the rate of increase in cell proliferation

NADH, through CtBP, represses CDKN1A and causes cell cycle progression. Thus, the rate of NADH-increase increases the cell proliferation rate through the cell cycle, working as the positive arm of the feedback loop (Fig. 1b). On the other hand, NAD⁺ is required for glycolysis, which is required for the continued increase in cell proliferation rate. Thus, a continued increase in cell proliferation rate requires higher and higher conversion of NADH to NAD⁺, reducing the rate of NADH increase and working as the negative arm of the loop (Fig. 1b).

Model

The cytosolic/nuclear NADH regulates the cellular processes through the C-terminal binding protein (CtBP). CtBP is a global corepressor that forms repressor complexes with other corepressors in the presence of NADH^{51,52}. CtBP represses CDKN1A⁷, a universal inhibitor of cyclin kinases⁵³, causing cell cycle progression (Fig. 1a). Thus, cell proliferation increases with the increase in NADH concentration. The dependence of the rate of increase of cell proliferation, C_p , on NADH concentration, N , can be given by Hill's function for a positive regulation. The positive regulation of the cell proliferation rate can also be given by the Michaelis-Menten kinetics in which the cell proliferation C_p works as an enzyme and NADH concentration, N , takes the place of a substrate. The growth rate also decreases due to apoptosis. Thus, the rate of change in cell proliferation, C_p , is given as:

$$\frac{dC_p}{dt} = \frac{k_1 C_p N}{k_2 + N} - k_{d1} C_p \quad (14)$$

where, k_1 , k_2 , and k_{d1} are parameters, C_p is the cell proliferation, and N is the NADH concentration. Cell proliferation C_p is defined as the fold increase in the number of cells from a single cell. The parameter k_1 represents the NADH-dependent cell division caused by the repression of CDKN1A by CtBP-NADH. The parameter k_2 represents NADH-independent apoptosis, while the addition of N in the denominator $k_2 + N$ is due to the NADH-dependent apoptosis caused by the accumulation of TP53 and the decrease in CDKN1A by NADH. Further, as a normal regulatory mechanism in cells, an increase in the proliferation rate is countered by the cell cycle-dependent apoptosis caused by the tumor-suppressor genes such as TP53 and RB1⁵⁴. The parameter k_{d1} represents the cell cycle-dependent apoptosis. The parameter k_2 represents the basal level of apoptosis. It can be measured when NADH concentration in the cell is not externally altered. On the other hand, NADH concentration in the cell can be increased by inhibiting NADH oxidases and apoptosis can be measured. Thus, the proportionality constant between an increase in NADH concentration and the rate of apoptosis can be measured for calculating the value of $k_2 + N$ in the denominator of Eq. 14. Similarly, the rate of cell cycle progression can be increased and the rate of apoptosis caused by the increase in cell cycle can be calculated to find the value of the constant k_{d1} .

Equation 14 is based on the precondition that all cells will conduct mitotic division, generating identical progeny cells after each mitotic cycle, which is true among normal stem cells. However, malignant cells exhibit disordered mitotic cycles, i.e., non-canonical mitosis, such as entering endocycles, yielding polyploid cells containing multiple copies of the genome with a simultaneously enlarged cell body. These cells may retain a similar NADH concentration in Eq. 14. However, C_p is the fold increase in the cell number from a single cell. In the case of endocycles, we need to define cell mass C_m , which is the fold increase in the cell mass from a single cell mass. C_m is proportional to C_p . We will have to determine the proportionality constant to convert C_p into C_m and vice versa.

Glycolysis produces NADH, increasing cell proliferation through CtBP and CDKN1A (Fig. 1a). On the other hand, NADH inhibits continued glycolysis by inhibiting GAPDH. Further, the onward oxidation of NADH to generate lactate helps unblock glycolysis through the pyruvate-to-lactate conversion reaction, which decreases NADH. This decrease lowers the

overall rate of increase of NADH with aerobic glycolysis. Thus, a higher and higher cell proliferation causes a lower and lower increase in NADH, i.e., a continued increase in cell proliferation gives a diminishing return of the rate of increase of NADH in the cytoplasm. Therefore, there is a negative regulation of the rate of increase of NADH in the cells by the cell proliferation, C_p .

We denote the NADH flux from glycolysis as k_3 and fold decrease in this flux due to pyruvate-to-lactate conversion reaction as k_4 . This fold decrease is augmented by dilution in the NADH concentration due to cell proliferation C_p , which is defined as the fold increase in the number of cells from a single cell. Thus, the rate of increase in NADH concentration, by taking into account the glycolysis, the pyruvate-to-lactate conversion reaction, and the dilution due to the cell proliferation, is given as $\frac{k_3}{k_4 + C_p}$, which is also the Hill's function for the negative regulation of the NADH rate by cell proliferation (Fig. 1b). Further, the flux of NADH and NADH-equivalent is also diverted to mitochondria for oxidative phosphorylation and TCA cycle, respectively. We assume that the flux of NADH and NADH-equivalent to mitochondria follows a first-order kinetics and is, thus, given as $k_{d2}N$, where $\frac{1}{k_{d2}}$ is the resistance of the NADH and NADH-equivalent flux to mitochondria. Thus, the rate of change of NADH concentration in the cytoplasm by taking into account the generation of NADH in the cytoplasm and removal from the cytoplasm is given as:

$$\frac{dN}{dt} = \frac{k_3}{k_4 + C_p} - k_{d2}N \quad (15)$$

where, k_{d2} is a parameter.

The positive regulation of the proliferation rate by NADH-CtBP and negative regulation of NADH by the cell proliferation makes a negative feedback loop between the cell proliferation rate and the rate of NADH increase (Fig. 1b). This negative feedback loop is the key to resolving the Warburg effect.

From Eq. 14, at the steady state,

$$N = \frac{k_1 k_2}{k_1 - k_{d1}} \quad (16)$$

Thus, NADH concentration in the cytoplasm is controlled by the parameters of the cell cycle and apoptosis.

Further, from Eq. 15, at the steady state,

$$C_p = \frac{k_3}{k_{d2}N} - k_4 \quad (17)$$

Thus, an increase in the NADH concentration decreases cell proliferation, a consequence of the negative feedback loop between cell proliferation and NADH concentration in the cytoplasm (Fig. 1b).

Let $r = \frac{NADH}{NAD^+}$, then from Eq. 17 at the steady state (Supplementary Information 3),

$$\frac{C_p}{C_{p0}} = \frac{\left(\frac{k_3}{k_4 k_{d2} N_0}\right) \left(\frac{r+1}{r_0+1}\right) \frac{r_0}{r} - 1}{\left(\frac{k_3}{k_4 k_{d2} N_0}\right) - 1} \quad (18)$$

where C_{p0} is the cell proliferation at the NADH/NAD⁺ ratio of r_0 when NADH concentration is N_0 (the baseline) and C_p is the cell proliferation when the NADH/NAD⁺ ratio is r .

We denote the ratio $\frac{k_3}{k_4 k_{d2} N_0}$ as the inverse-of-the potential-to-proliferation-increase (IPPI). Thus,

$$IPPI = \frac{k_3}{k_4 k_{d2} N_0} \quad (19)$$

From Eq. 17, an increase in k_4 , the fold decrease in the incoming NADH flux from glycolysis due to the pyruvate-to-lactate conversion

reaction, decreases cell proliferation. Similarly, an increase in k_{d2} , representing oxidative phosphorylation, decreases the proliferation, while an increase in k_3 , representing the increase in NADH flux due to the upstream steps in glycolysis, increases cell proliferation. Thus, based on this basic underlying motif (Fig. 1b), on an absolute basis, the pyruvate-to-lactate conversion reaction and oxidative phosphorylation do not help promote cell proliferation if they were not required to provide metabolites for the anabolic reactions required for cell proliferation because the cytoplasmic NADH through CtBP can cause the cell cycle progression, suggesting that the presence of mitochondria is not helpful for an organism's proliferation.

However, Eq. 17 also shows that a decrease in the NADH concentration, N increases the cell proliferation. Thus, on a relative basis, the processes that help reduce the NADH concentration in the cytoplasm can help increase cells' proliferation. In agreement, from Eq. 18, on a relative basis, the pyruvate-to-lactate conversion reaction and oxidative phosphorylation help cells attain a higher cell proliferation (the results section) when the NADH/NAD⁺ ratio decreases. Thus, carcinogenesis may use aerobic glycolysis to attain a higher, relative cell proliferation through a decrease in NADH/NAD⁺ ratio while oxidative phosphorylation plays a synergistic role.

The parameters of the model

The only important parameter in this model is in the form of a non-dimensional number, $\frac{k_3}{k_4 k_{d2} N_0}$, which is denoted as the inverse-of-the-potential-to-proliferation-increase (IPPI) (Figs. 2c and 3a, b).

From Eq. 17, the cells are quiescent ($C_{p0} = 0$) for IPPI = 1. Further, when IPPI > 1, cells have a positive proliferation $C_{p0} > 0$ from Eq. 17. In contrast, when IPPI < 1, the cells have a negative proliferation $C_{p0} < 0$ from Eq. 17.

When IPPI > 1, i.e., when the baseline proliferation is positive, and when $r \ll 1$ and $r_0 \ll 1$ (NADH/NAD⁺ ratio varies from 1/700 to 1/60³³ in eukaryotic cells),

$$\left(\frac{r+1}{r_0+1}\right) \approx 1 \tag{20}$$

then, as r decreases, i.e., $r < r_0$, $C_p > C_{p0}$ from Eq. 18. Thus, from Eq. 18, for IPPI > 1 and $r_0 \ll 1$, as NADH/NAD⁺ ratio decreases, the cell proliferation increases above the baseline value.

In contrast, when $r \gg 1$ and $r_0 \gg 1$, $\left(\frac{r+1}{r_0+1}\right) \frac{r_0}{r} = 1$ in Eq. 18. Thus, $\frac{C_p}{C_{p0}} = 1$, from Eq. 18, when $r \gg 1$ and $r_0 \gg 1$. Thus, when NADH is much higher than NAD⁺ in the cells, the cells' proliferation is invariant. Therefore, in the result section, we only considered the physically realistic case of $r \ll 1$ and $r_0 \ll 1$. Further, we only considered the case when IPPI ≥ 1 because the baseline cell proliferation is non-negative under this condition. Thus, our results above are generally valid for $r \ll 1$ and $r_0 \ll 1$, and IPPI ≥ 1 .

Under the above conditions, as shown in the result section, a lower value of IPPI is more potent in increasing the relative cell proliferation, i.e., in increasing the ratio, $\frac{C_p}{C_{p0}}$, when the NADH/NAD⁺ ratio decreases. Further, since IPPI is a ratio of the process that increases NADH (i.e., k_3 or the incoming NADH flux from glycolysis) to the processes that decrease NADH (i.e., the product of k_4 or the fold decrease in the incoming NADH flux from glycolysis due to the pyruvate-to-lactate conversion reaction and k_{d2} . N or the outgoing NADH flux to oxidative phosphorylation) and since a lower value of IPPI is more potent in increasing the cell proliferation (the results section), the retention of the reducing power of NADH in the cytoplasm is detrimental to the increase in the relative cell proliferation. Below, we define the dimensionless parameter, IPPI, as:

$$\text{IPPI} = \frac{\text{Incoming NADH flux from glycolysis}(k_3)}{\text{Product of the fold reduction in the incoming NADH flux from glycolysis due to pyruvate - to - lactate conversion reaction}(k_4)\text{and the outgoing NADH flux to oxidative phosphorylation}(k_{d2}N_0)} \tag{21}$$

Reporting summary

Further information on research design is available in the Nature Research Reporting Summary linked to this article.

Data availability

All data supporting the findings of this study are available within the paper and its Supplementary Information.

Code availability

Computer code will be made available upon request.

Received: 19 October 2023; Accepted: 29 April 2024;

Published online: 24 May 2024

References

- Heiden, M. G. V., Cantley, L. C. & Thompson, C. B. Understanding the warburg effect: The metabolic requirements of cell proliferation. *Science* **324**, 1029–1033 (2009).
- Warburg, O. On the origin of cancer cells. *Science* **123**, 309–314 (1956).
- Wang, Y. et al. Saturation of the mitochondrial NADH shuttles drives aerobic glycolysis in proliferating cells. *Mol. Cell* **82**, 3270–3283.e9 (2022).
- Birts, C. N. et al. p53 is regulated by aerobic glycolysis in cancer cells by the CtBP family of NADH-dependent transcriptional regulators. *Sci. Signal* **13**, eaau9529 (2020).
- Hanse, E. A. et al. Cytosolic malate dehydrogenase activity helps support glycolysis in actively proliferating cells and cancer. *Oncogene* **36**, 3915–3924 (2017).
- Somasundaram, K. et al. Arrest of the cell cycle by the tumour-suppressor BRCA1 requires the CDK-inhibitor p21WAF1/Cip1. *Nature* **389**, 187–190 (1997).
- Yu, Y. et al. RBBP8/CtIP suppresses P21 expression by interacting with CtBP and BRCA1 in gastric cancer. *Oncogene* **39**, 1273–1289 (2019).
- Zhang, Q., Piston, D. W. & Goodman, R. H. Regulation of corepressor function by nuclear NADH. *Science* **295**, 1895–1897 (2002).
- Karimian, A., Ahmadi, Y. & Yousefi, B. Multiple functions of p21 in cell cycle, apoptosis and transcriptional regulation after DNA damage. *DNA Repair (Amst.)* **42**, 63–71 (2016).
- Pilié, P. G., Tang, C., Mills, G. B. & Yap, T. A. State-of-the-art strategies for targeting the DNA damage response in cancer. *Nat. Rev. Clin. Oncol.* **16**, 81–104 (2018).
- Battle, E. & Clevers, H. Cancer stem cells revisited. *Nat. Med.* **23**, 1124–1134 (2017).
- Lee, S. H., Reed-Newman, T., Anant, S. & Ramasamy, T. S. Regulatory Role of Quiescence in the Biological Function of Cancer Stem Cells. *Stem Cell Rev. Rep.* **16**, 1185–1207 (2020).
- Chen, W., Dong, J., Haiech, J., Kilhoffer, M. C. & Zeniou, M. Cancer stem cell quiescence and plasticity as major challenges in cancer therapy. *Stem Cells Int* **2016**, 1740936 (2016).
- McConnell, A. M. et al. p53 Regulates Progenitor Cell Quiescence and Differentiation in the Airway. *Cell Rep.* **17**, 2173–2182 (2016).
- Nakamura-Ishizu, A., Takizawa, H. & Suda, T. The analysis, roles and regulation of quiescence in hematopoietic stem cells. *Development* **141**, 4656–4666 (2014).
- Hebert-Chatelain, E. et al. Preservation of NADH ubiquinone-oxidoreductase activity by Src kinase-mediated phosphorylation of NDUFB10. *Biochim. et. Biophys. Acta (BBA) - Bioenerg.* **1817**, 718–725 (2012).
- Krymskaya, V. P. et al. Src is necessary and sufficient for human airway smooth muscle cell proliferation and migration. *FASEB J.* **19**, 1–20 (2005).
- Je, D. W., O, Y. M., Ji, Y. G., Cho, Y. & Lee, D. H. The inhibition of Src family kinase suppresses pancreatic cancer cell proliferation, migration, and invasion. *Pancreas* **43**, 768–776 (2014).

19. Niu, G. et al. Roles of activated Src and Stat3 signaling in melanoma tumor cell growth. *Oncogene* **21**, 7001–7010 (2002). *2002* 21:46.
20. Summy, J. M. & Gallick, G. E. Src family kinases in tumor progression and metastasis. *Cancer Metast. Rev.* **22**, 337–358 (2003).
21. Gu, H. et al. MDH1-mediated malate-aspartate NADH shuttle maintains the activity levels of fetal liver hematopoietic stem cells. *Blood* **136**, 553–571 (2020).
22. Cheng, S. C. et al. mTOR- and HIF-1 α -mediated aerobic glycolysis as metabolic basis for trained immunity. *Science* **345**, 1250684 (2014). (1979).
23. Masuda, Y., Togo, T., Mizuno, S., Konishi, M. & Nanba, H. Soluble β -glucan from *Grifola frondosa* induces proliferation and Dectin-1/Syk signaling in resident macrophages via the GM-CSF autocrine pathway. *J. Leukoc. Biol.* **91**, 547–556 (2012).
24. Saeed, S. et al. Epigenetic programming of monocyte-to-macrophage differentiation and trained innate immunity. *Science* **345**, 1251086 (2014).
25. Demir, G., Klein, H. O., Mandel-Molinas, N. & Tuzuner, N. Beta glucan induces proliferation and activation of monocytes in peripheral blood of patients with advanced breast cancer. *Int Immunopharmacol.* **7**, 113–116 (2007).
26. Baixauli, F. et al. An LKB1-mitochondria axis controls TH17 effector function. *Nature* **610**, 555–561 (2022).
27. Ansó, E. et al. The mitochondrial respiratory chain is essential for haematopoietic stem cell function. *Nat. Cell Biol.* **19**, 614–625 (2017).
28. Ancel, S., Stuelsatz, P. & Feige, J. N. Muscle Stem Cell Quiescence: Controlling Stemness by Staying Asleep. *Trends Cell Biol.* **31**, 556–568 (2021).
29. Chesnelong, C. et al. Lactate dehydrogenase A silencing in IDH mutant gliomas. *Neuro. Oncol.* **16**, 686–695 (2014).
30. Seltzer, M. J. et al. Inhibition of glutaminase preferentially slows growth of glioma cells with mutant IDH1. *Cancer Res* **70**, 8981–8987 (2010).
31. Shibahara, I. et al. Malignant clinical features of anaplastic gliomas without IDH mutation. *Neuro. Oncol.* **17**, 136–144 (2015).
32. Antonica, F. et al. A slow-cycling/quiescent cells subpopulation is involved in glioma invasiveness. *Nat. Commun.* **13**, 1–15 (2022).
33. Yang, Y. & Sauve, A. A. NAD⁺ metabolism: Bioenergetics, signaling and manipulation for therapy. *Biochim Biophys. Acta* **1864**, 1787 (2016).
34. Lim, J. H. et al. Sirtuin 1 Modulates Cellular Responses to Hypoxia by Deacetylating Hypoxia-Inducible Factor 1 α . *Mol. Cell* **38**, 864–878 (2010).
35. Go, S., Kramer, T. T., Verhoeven, A. J., Oude Elferink, R. P. J. & Chang, J. C. The extracellular lactate-to-pyruvate ratio modulates the sensitivity to oxidative stress-induced apoptosis via the cytosolic NADH/NAD⁺ redox state. *Apoptosis* **26**, 38–51 (2021).
36. Gartel, A. L. & Tyner, A. L. The Role of the Cyclin-dependent Kinase Inhibitor p21 in Apoptosis 1.
37. Liu, Y. et al. p53 Regulates Hematopoietic Stem Cell Quiescence. *Cell Stem Cell* **4**, 37–48 (2009).
38. La, T. et al. A p53-responsive miRNA network promotes cancer cell quiescence. *Cancer Res* **78**, 6666–6679 (2018).
39. Lee, J. et al. Runx1 and p21 synergistically limit the extent of hair follicle stem cell quiescence in vivo. *Proc. Natl Acad. Sci. USA* **110**, 4634–4639 (2013).
40. Lee, D. C. et al. A Lactate-Induced Response to Hypoxia. *Cell* **161**, 595–609 (2015).
41. Ivashkiv, L. B. The hypoxia–lactate axis tempers inflammation. *Nat. Rev. Immunol.* **20**, 85–86 (2019).
42. Brisson, L. et al. Lactate Dehydrogenase B Controls Lysosome Activity and Autophagy in Cancer. *Cancer Cell* **30**, 418–431 (2016).
43. Rzymiski, T. et al. Regulation of autophagy by ATF4 in response to severe hypoxia. *Oncogene* **29**, 4424–4435 (2010).
44. García-Prat, L. et al. Autophagy maintains stemness by preventing senescence. *Nature* **529**, 37–42 (2016).
45. Pan, H., Cai, N., Li, M., Liu, G. H. & Izpisua Belmonte, J. C. Autophagic control of cell ‘stemness’. *EMBO Mol. Med* **5**, 327–331 (2013).
46. Sbrana, F. V. et al. The Role of Autophagy in the Maintenance of Stemness and Differentiation of Mesenchymal Stem Cells. *Stem Cell Rev. Rep.* **12**, 621–633 (2016).
47. García-Prat, L., Sousa-Victor, P. & Muñoz-Cánoves, P. Proteostatic and Metabolic Control of Stemness. *Cell Stem Cell* **20**, 593–608 (2017).
48. van den Beucken, T. et al. Hypoxia promotes stem cell phenotypes and poor prognosis through epigenetic regulation of DICER. *Nat. Commun.* **5**, 1–13 (2014).
49. Zhu, P. et al. A novel hypoxic long noncoding RNA KB-1980E6.3 maintains breast cancer stem cell stemness via interacting with IGF2BP1 to facilitate c-Myc mRNA stability. *Oncogene* **40**, 1609–1627 (2021).
50. Martin, A. & Cano, A. Tumorigenesis: Twist1 links EMT to self-renewal. *Nat. Cell Biol.* **12**, 924–925 (2010).
51. Fjeld, C. C., Birdsong, W. T. & Goodman, R. H. Differential binding of NAD⁺ and NADH allows the transcriptional corepressor carboxyl-terminal binding protein to serve as a metabolic sensor. *Proc. Natl Acad. Sci.* **100**, 9202–9207 (2003).
52. Jaiswal, A. & Singh, R. CtBP: A global regulator of balancing acts and homeostases. *Biochim. et. Biophys. Acta (BBA) - Rev. Cancer* **1878**, 188886 (2023).
53. Xiong, Y. et al. p21 is a universal inhibitor of cyclin kinases. *Nature* **366**, 701–704 (1993).
54. Pucci, B., Kasten, M. & Giordano, A. Cell Cycle and Apoptosis. *Neoplasia* **2**, 291–299 (2000).

Author contributions

R.S. conceptualized the manuscript. A.J. and R.S. prepared the mathematical model. A.J. and R.S. analyzed the results. R.S. wrote the manuscript.

Competing interests

The authors declare no competing interests.

Additional information

Supplementary information The online version contains supplementary material available at

<https://doi.org/10.1038/s41540-024-00377-x>.

Correspondence and requests for materials should be addressed to Raghvendra Singh.

Reprints and permissions information is available at <http://www.nature.com/reprints>

Publisher's note Springer Nature remains neutral with regard to jurisdictional claims in published maps and institutional affiliations.

Open Access This article is licensed under a Creative Commons Attribution 4.0 International License, which permits use, sharing, adaptation, distribution and reproduction in any medium or format, as long as you give appropriate credit to the original author(s) and the source, provide a link to the Creative Commons licence, and indicate if changes were made. The images or other third party material in this article are included in the article's Creative Commons licence, unless indicated otherwise in a credit line to the material. If material is not included in the article's Creative Commons licence and your intended use is not permitted by statutory regulation or exceeds the permitted use, you will need to obtain permission directly from the copyright holder. To view a copy of this licence, visit <http://creativecommons.org/licenses/by/4.0/>.

© The Author(s) 2024